Lecture 8

nucleon structure, parton tomography, and nucleon mass

outline:

reminder of deep inelastic scattering

going exclusive: deeply virtual Compton scattering

some experimental considerations and presently running campaigns

tomography

the Electron-Ion Collider EIC

the nucleon mass puzzle: mass without mass

DEEP INELASTIC SCATTERING

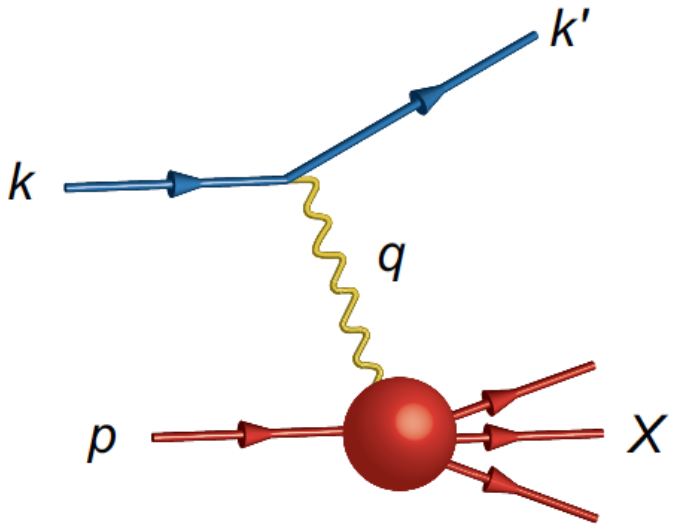

- k, k': four momenta of the incoming and outgoing lepton (e,μ)
- p: four momentum of the nucleon (proton, neutron)
- squared momentum transfer: $Q^2 = -q^2 = (k-k')^2$
- Bjorken variable: $x = Q^2/(2p\cdot q)$, $0 < x < 1$
- inelasticity $y = (q\cdot p) / (k\cdot p)$, $0 < y < 1$
- squared invariant mass of hadronic system X: $W^2 = (p+q)^2$

slide from lecture 6, only k' is measured
example of inclusive reaction

deeply virtual Compton scattering (DVCS)

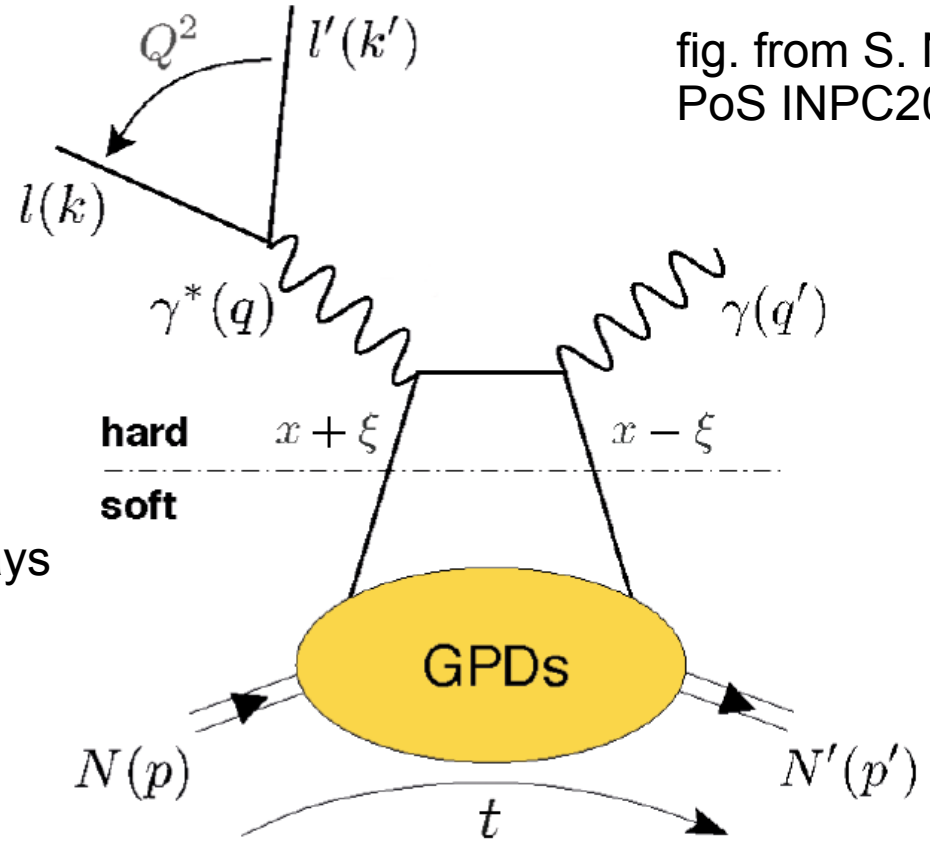

fig. from S. Niccolai,
PoS INPC2016 (2017) 368

note: opposite to the case of deep inelastic scattering, the final proton stays intact

The handbag diagram for the DVCS process on the nucleon $\ell N \to \ell' N' \gamma$. The four-momenta of the incoming and outgoing leptons are labeled as, respectively, k and k', while those of the virtual and real photons are indicated by, respectively, q and q'. x is the average longitudinal-momentum fraction of the struck parton, and 2ξ is the difference of longitudinal-momentum fractions between the initial and the final parton. $t = (p - p')^2$ is the squared four-momentum transfer between the initial and final nucleon.

generalized parton distributions (GPD) instead of electric and magnetic form factors

Considering only quark-helicity-conserving processes, which are dominant for DVCS, at leading order and at leading twist the reaction is described by four GPDs, H^f, $\tilde{H}^f$, E^f, $\tilde{E}^f$ (where f stands for a light quark or for a gluon g, in which case the DVCS diagram differs from that of fig. 1), that account for the possible combinations of relative orientations of nucleon spin and parton helicity between the initial and final states. The GPDs H and E do not depend on the parton helicity and are therefore called unpolarized GPDs, while $\tilde{H}$ and $\tilde{E}$ depend on the parton helicity and are called polarized GPDs. The GPDs H and $\tilde{H}$ conserve the spin of the nucleon, whereas E and $\tilde{E}$ correspond to a nucleon-spin flip.

text taken from:

Nicole d'Hose, Silvia Niccolai, Armine Rostomyan, Eur. Phys. J. A (2016) **52**: 151

parameters in the GPDs

instead of the variables x_B and Q^2, the GPD depend on three parameters:

x, ζ, t as defined in the DVCS figure

because of the vector nature of (p-p'), this implies in addition to | t |, one (two) angle(s) for the case of scattering of an unpolarized (polarized) target.

Evaluated in the frame in which the 3-momentum of p and p' are very large (Breit frame) this implies:

$t = (p - p')^2 = 2 E_p E_{p'} (1-\cos(\theta)) = - 4 E_p E_{p'} \sin^2(\theta/2)$

$\sqrt{(-t)} = 2 | \mathbf{p} | \sin(\theta/2) = q_T$ = transverse momentum transfer to the proton

$2\zeta = (x+\zeta) - (x-\zeta)$
2ζ = difference in momentum fractions of the initial and final proton

parameters in the GPDs

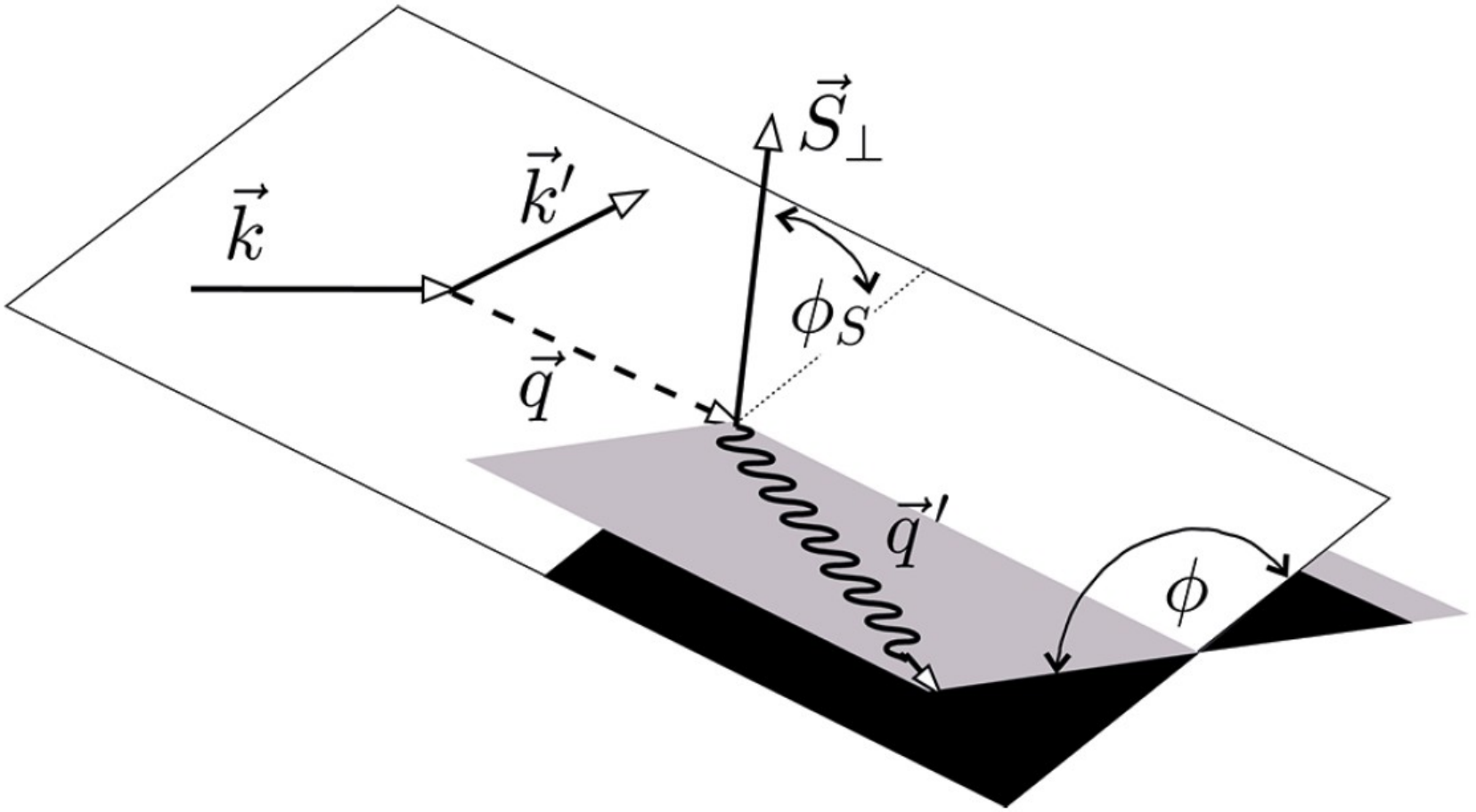

Scheme illustrating the definition of the angles ϕ, formed by the leptonic and hadronic planes, and ϕ_S formed by the lepton scattering plane and $\vec{S}_\perp$, the component of the target polarization vector that is orthogonal to $\vec{q}$.

A note on factorization

separating the soft, non-perturbative sector where form factors and, hence, PDF's and GPD's come into the game, from the hard, perturbative sector where precise QCD based calculations can be performed

a detailed analysis is beyond what we can describe in this lecture, see: Collins and Freund, Phys.Rev.D 59 (1999) 074009

factorization proven for $-t << Q^2$
not easy to achieve since $t = (p - p')^2 = (q - q')^2$ see next slide, need large photon energy and large Q

alternate view: with momenta of struck partons, fig. from Ji and Bakker,

Nuclear Physics B (Proc. Suppl.) 251–252 (2014) 75–80

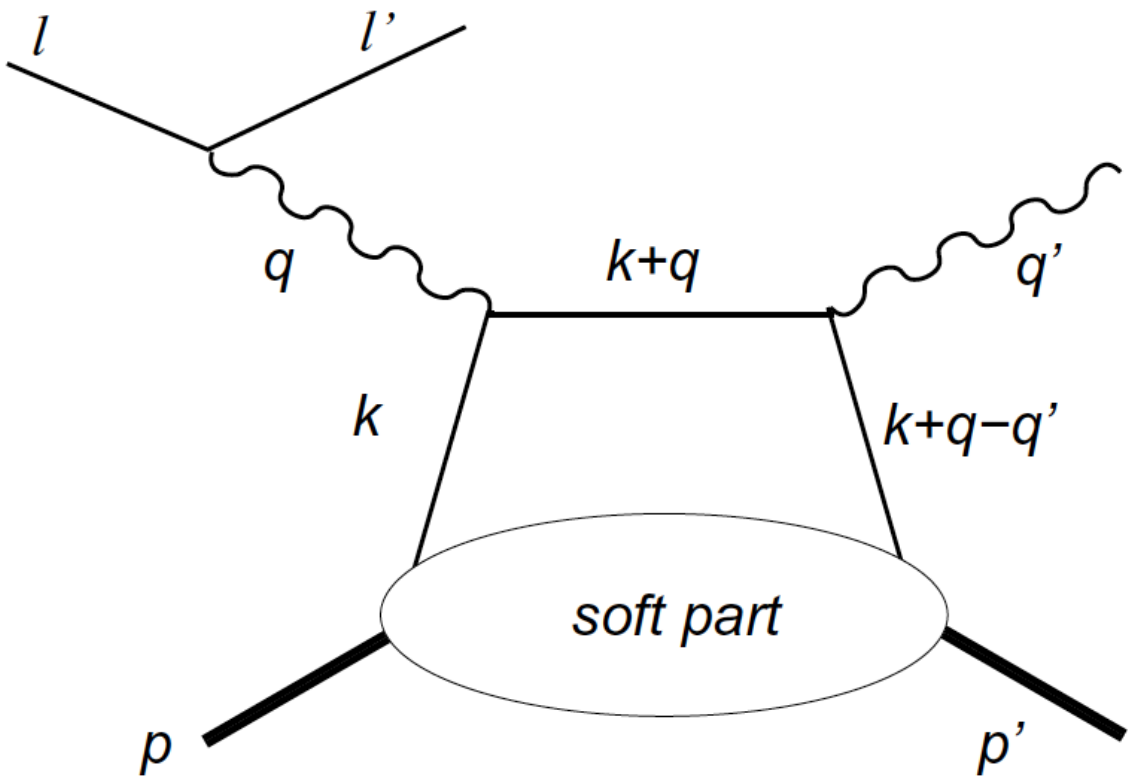

1: Complete handbag diagram for s-channel Virtual Compton scattering. A quark with momentum k is hit by a virtual photon with momentum q. The final, real photon has momentum q'.

then: p-k + (k+q-q') = p' ⟶ p – p' = q – q'

measurement of electron and real photon determines the complete kinematics

now adding the Bethe-Heitler contribution

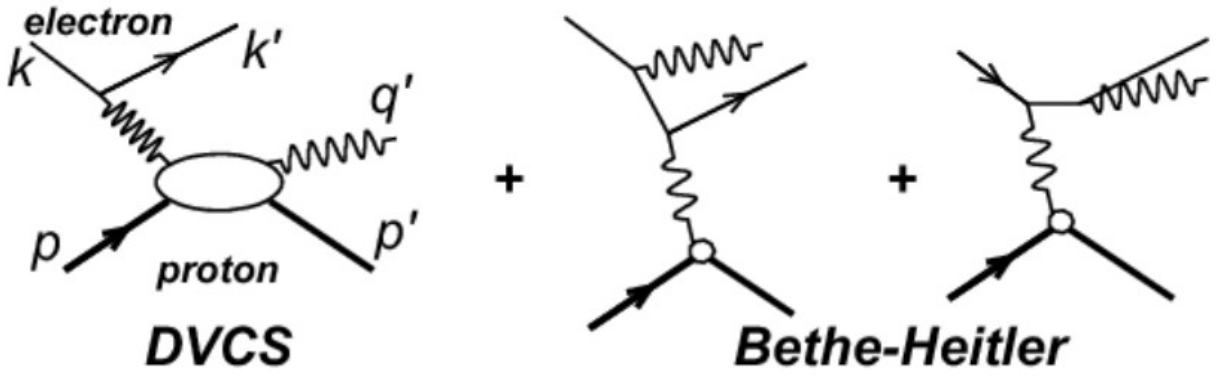

the purely electromagnetic Bethe-Heitler process is indistinguishable from the DVCS process, the two diagrams need to be added coherently

but: the Bethe-Heitler diagrams can be calculated with precision using QED

fig. from 1502.03246

now the idea of parton tomography

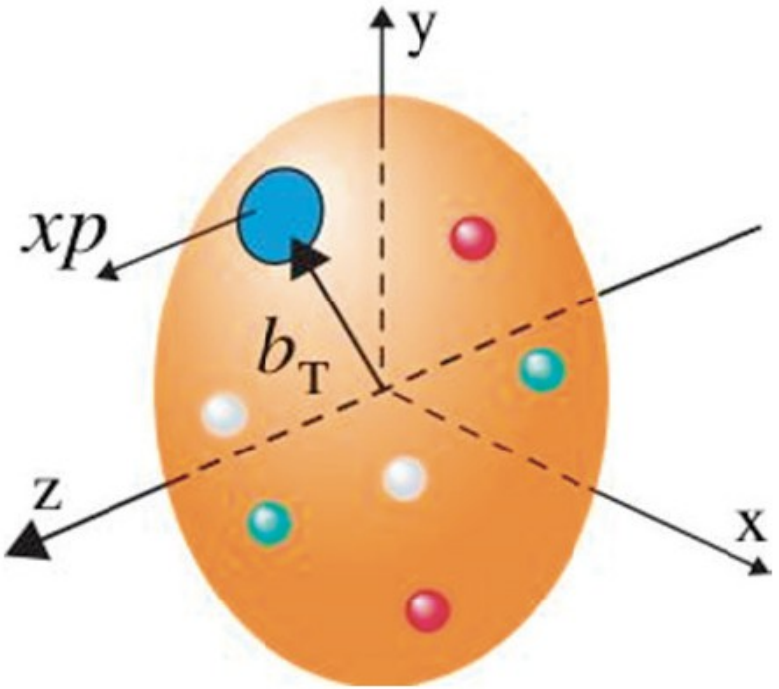

Schematic depiction of a nucleon containing a parton with longitudinal momentum xp and transverse position $b_T = (b_x, b_y)$. The z-direction is the beam direction. The transverse momentum (not shown) of the parton is $k_T = (k_x, k_y)$.
SOURCE: A. Accardi et al., 2016, Electron-ion collider: The next QCD frontier, *Eur. Phys. J. A* 52:268.

parton imaging – the key idea

The momentum transfer in DVCS to the final proton, characterized by $t = (p - p')^2 = (q - q')^2$ brings in a new kinematic variable t. The DVCS cross section depends on t. Since t is directly connected to the transverse component of the momentum transfer to the proton, this dependence contains information, via Fourier transformation, about the transverse position of the struck parton. Note that $\sqrt{(-t)} = 2 |\mathbf{p}| \sin(\theta/2)$ is the momentum transfer to the proton in the direction transverse to the motion of the proton, at least for small values of θ.

Through measurement and analysis of DVCS, the intend is to describe the structure of the nucleon in terms of the longitudinal momentum fraction and transverse position of its constituents, the quarks and gluons.

the DVCS cross section

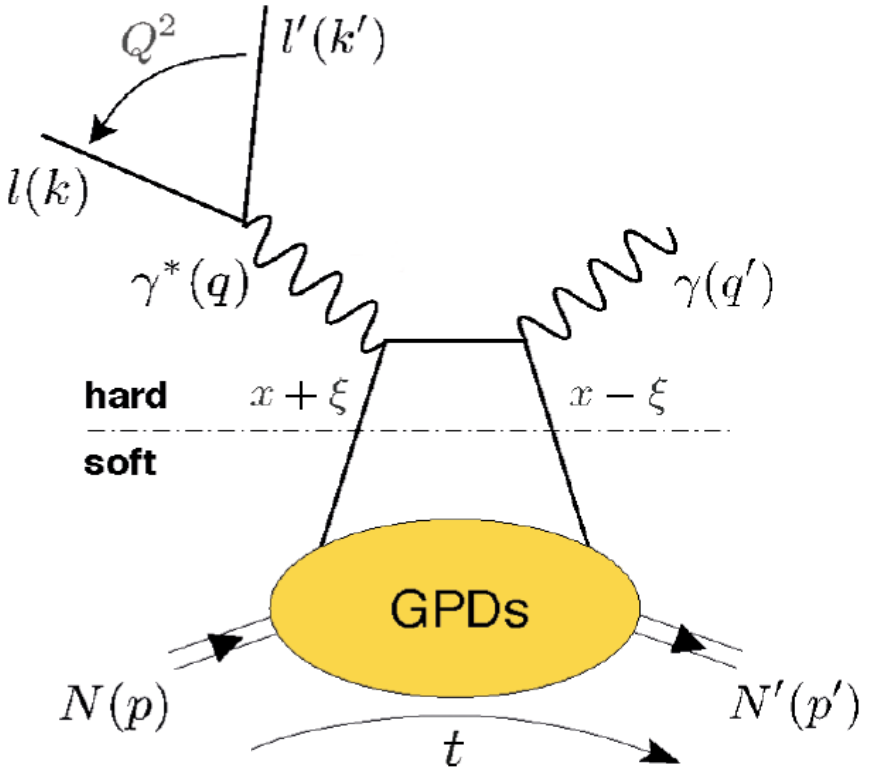

Chiral-even GPDs:
(helicity of parton conserved)

$H^{q,g}(x,\xi,t)$	$E^{q,g}(x,\xi,t)$	*for sum over parton helicities*
$\widetilde{H}^{q,g}(x,\xi,t)$	$\widetilde{E}^{q,g}(x,\xi,t)$	*for difference over parton helicities*
nucleon helicity conserved	*nucleon helicity changed*	

factorization for $|t|/Q^2 \ll 1$

imaging continued

- Nucleon tomography

$$q(x, \mathbf{b}_\perp) = \int \frac{\mathrm{d}^2\boldsymbol{\Delta}}{4\pi^2} e^{-i\mathbf{b}_\perp \cdot \boldsymbol{\Delta}} H^q(x, 0, t = -\boldsymbol{\Delta}^2)$$

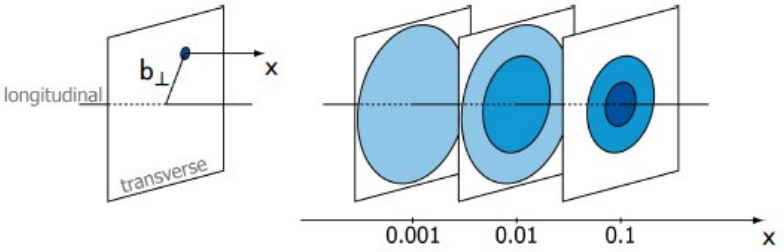

- Study of long. polarization with GPD $\tilde{H}$
- Study of distortion in transv. polarized nucleon with GPD E

- Impact parameter $\mathbf{b}_\perp$ defined w.r.t. center of momentum, such as $\sum x\,\mathbf{b}_\perp = 0$

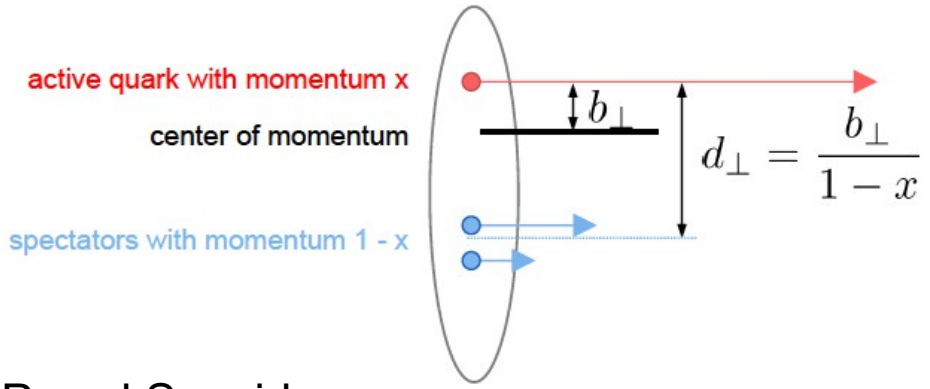

fig. from Pawel Sznajder

DVCS for real photon and real meson production

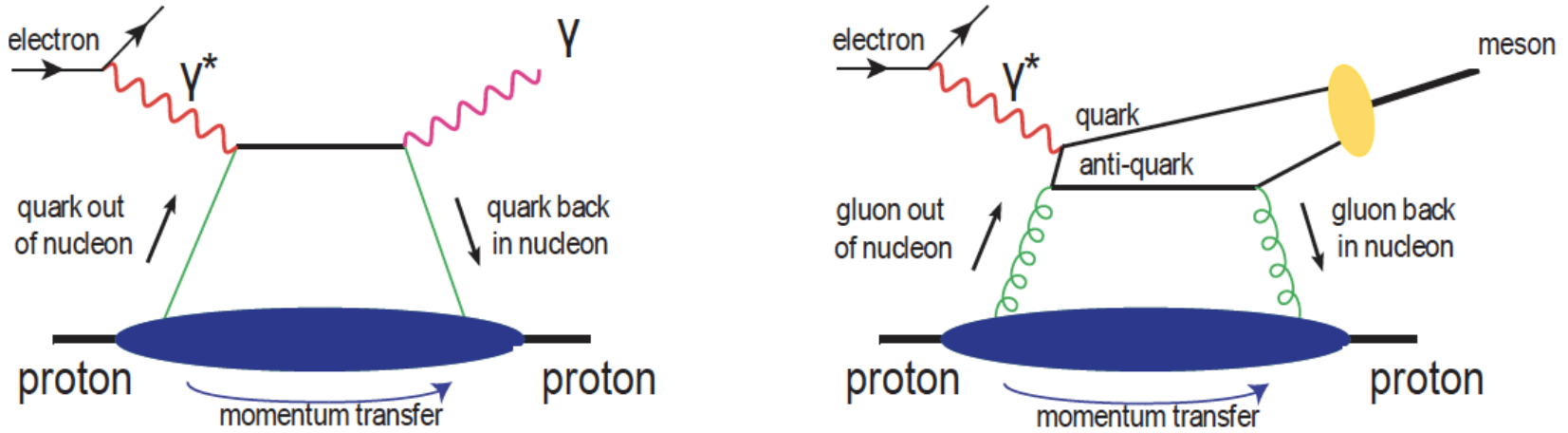

Real photon production (*left*) and real meson production (*right*). The virtual photon γ^* is emitted by the incoming electron. The final state photon and meson are real particles that can be observed in the detector. For the two-gluon process to dominate real meson production, the produced state should be heavy, like the J/ψ (a charm-anticharm quark bound state) or the Upsilon (Υ) particle (a bottom-antibottom quark bound state). In both processes, the nucleon remains intact but is deflected by a nonzero angle. SOURCE: Z.-E. Meziani.

using heavy meson production one can image also gluons

selected simulations and 1st experimental results

simulation of experiment at the future EIC, NAS report

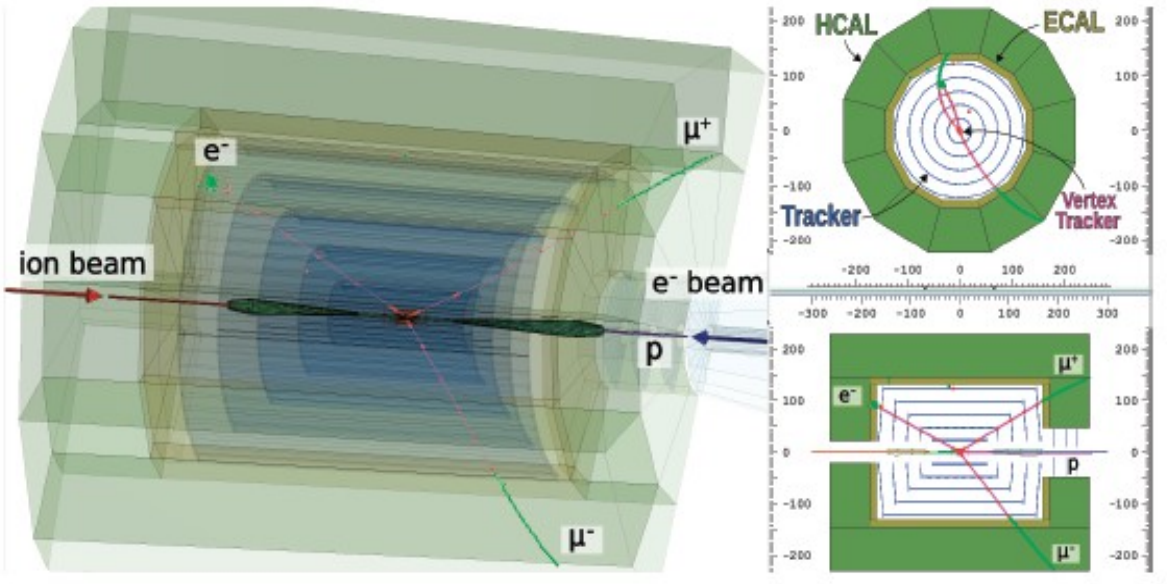

FIGURE 2.3 Simulated event display for real meson production in a design for an electron-ion colliding beam detector. The direction of the beams is indicated in the perspective (*left*) and side views (*lower right*). The upper-right panel shows a view along the beam direction. In this event, the colliding proton stays intact, and a heavy J/ψ meson is produced. The J/ψ decays into a pair of muons, which are detected together with the scattered electron. The scattered proton labeled p is close to the beam direction and detected in a separate detector farther from the interaction point. Events of this type are the basis of gluon tomography, as shown in Figure 2.5, and provide information on the gluon orbital angular momentum contribution to the nucleon spin. Similar events where an Upsilon ($b\bar{b}$) meson is produced on a proton close to "threshold," never before measured, will also help determine the gluon contributions to the mass of the nucleon. SOURCE: Argonne National Laboratory.

imaging the transverse size of gluons for different values of x

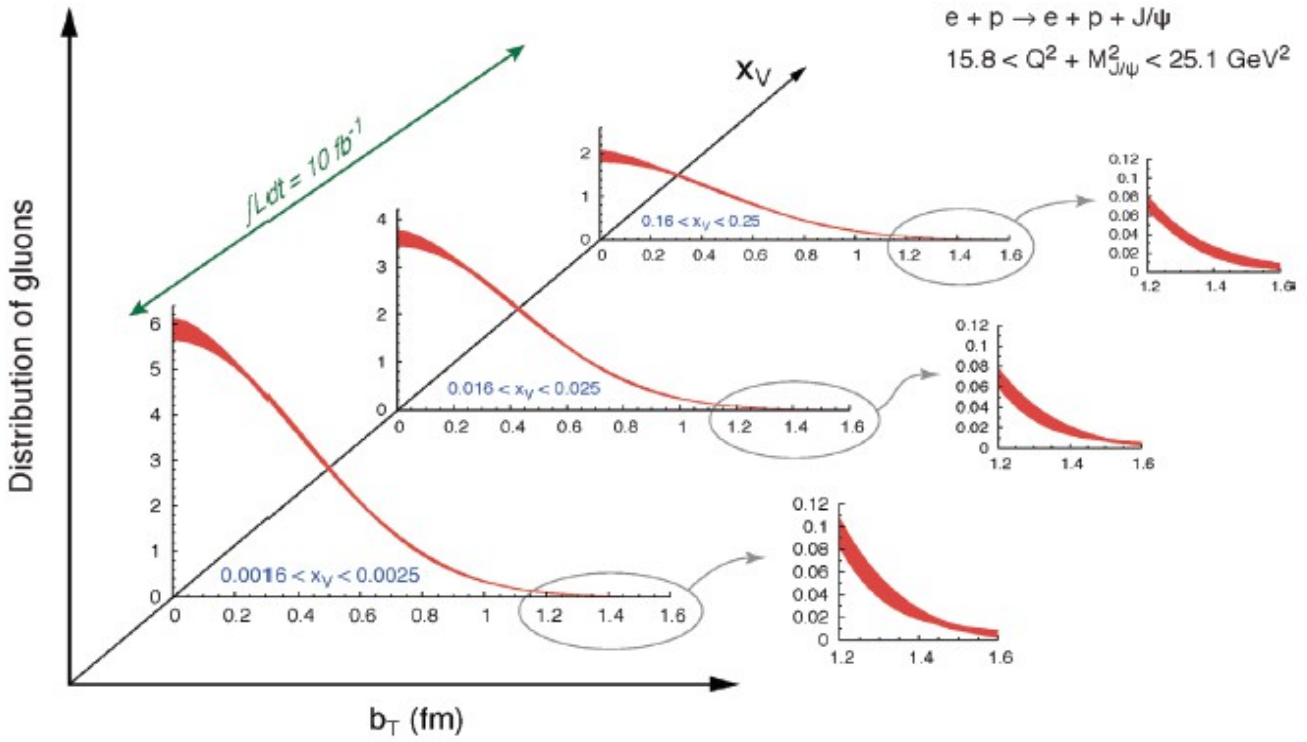

FIGURE 2.5 Gluon density distribution at several values of Bjorken *x*. An estimate of the precision that can be achieved using real meson production at an EIC is shown, based on an integrated luminosity of 10 fb^{-1}. The small insets illustrate the accuracy that can be achieved for large radii, relevant to the confinement problem. SOURCE: *Reaching for the Horizon*, 2015 DOE/NSF Long Range Plan for U.S. Nuclear Science.

now real data from Hera, Compass and JLAB

first HERA, at low x

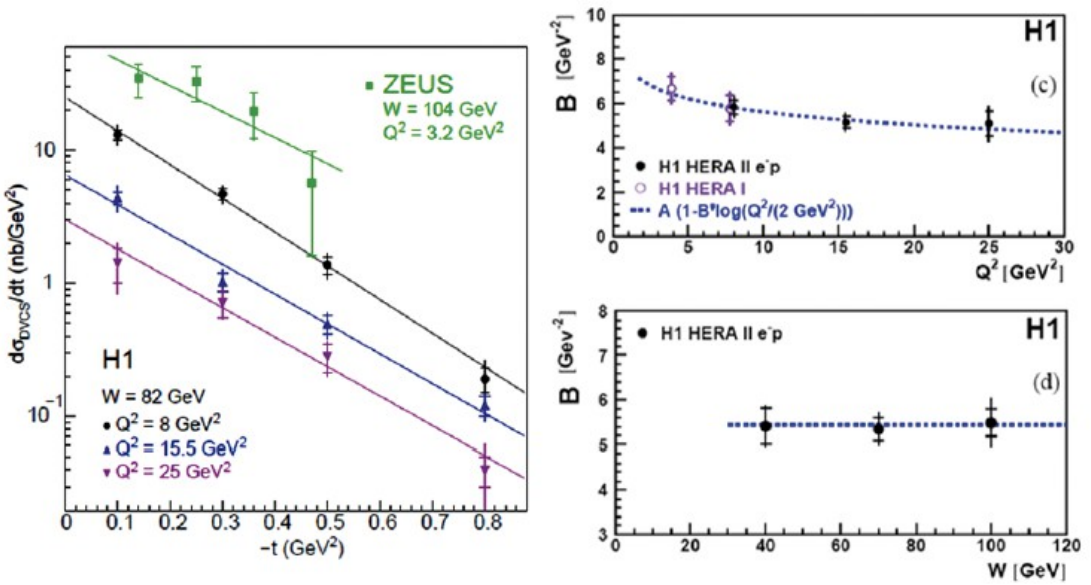

Fig. 5. Left: the t-dependence of the DVCS cross section for four values of Q^2, as measured by H1 and ZEUS. The curves are the results of fits of the form $e^{-B|t|}$. Right: the fitted B values as a function of Q^2 (top) and W (bottom). The curves represent the result of the fit $B(Q^2) = A(1 - B' \log(Q^2/2\,\mathrm{GeV}^2))$ (top) and the average value $B = 5.45\,\mathrm{GeV}^{-2}$ (bottom). Figure from ref. [32]. arXiv:0709.4114

expressed in spatial dimensions, this value of B corresponds to an rms size of the gluon distribution of r_{perp} = 0.65 ± 0.02 fm (= sqrt(2 B) 0.197) fm

now COMPASS data, arXiv:1802.02739

Akhunzyanov R *et al.* (COMPASS Collaboration) 2019 *Phys. Lett.* B **793** 188

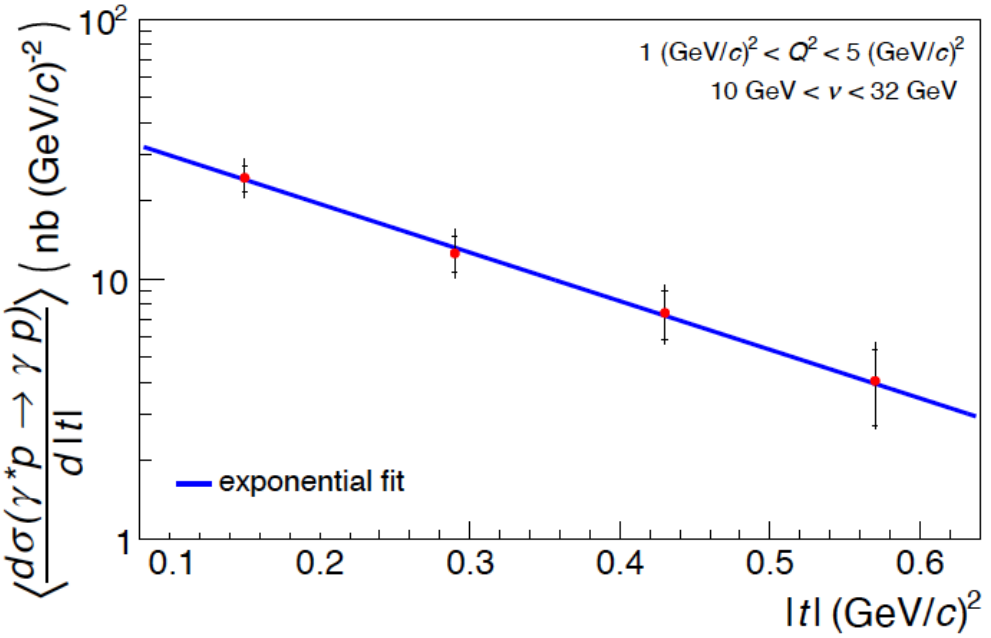

Differential DVCS cross section as a function of $|t|$. The mean value of the cross section is shown at the centre of each of the four $|t|$-bins. The blue curve is the result of a binned maximum likelihood fit of an exponential function to the data. This fit integrates the exponential model over the respective t-bins and does not use their central values, which are used for illustration only. The probability to observe a similar or better agreement of the data with the blue curve is approximately 7%. Here and in the next figure, inner error bars represent statistical uncertainties and outer error bars the quadratic sum of statistical and systematic uncertainties. Figure from Ref. [7].

$$B = (4.3 \pm 0.6_{\text{stat}} {}^{+\,0.1}_{-\,0.3}\big|_{\text{sys}}) \, (\text{GeV}/c)^{-2},$$

is obtained at the average kinematics $\langle W \rangle = 5.8\,\text{GeV}/c^2$, $\langle Q^2 \rangle = 1.8\,(\text{GeV}/c)^2$ and $\langle x_{\text{Bj}} \rangle = 0.056$

x dependence of B?

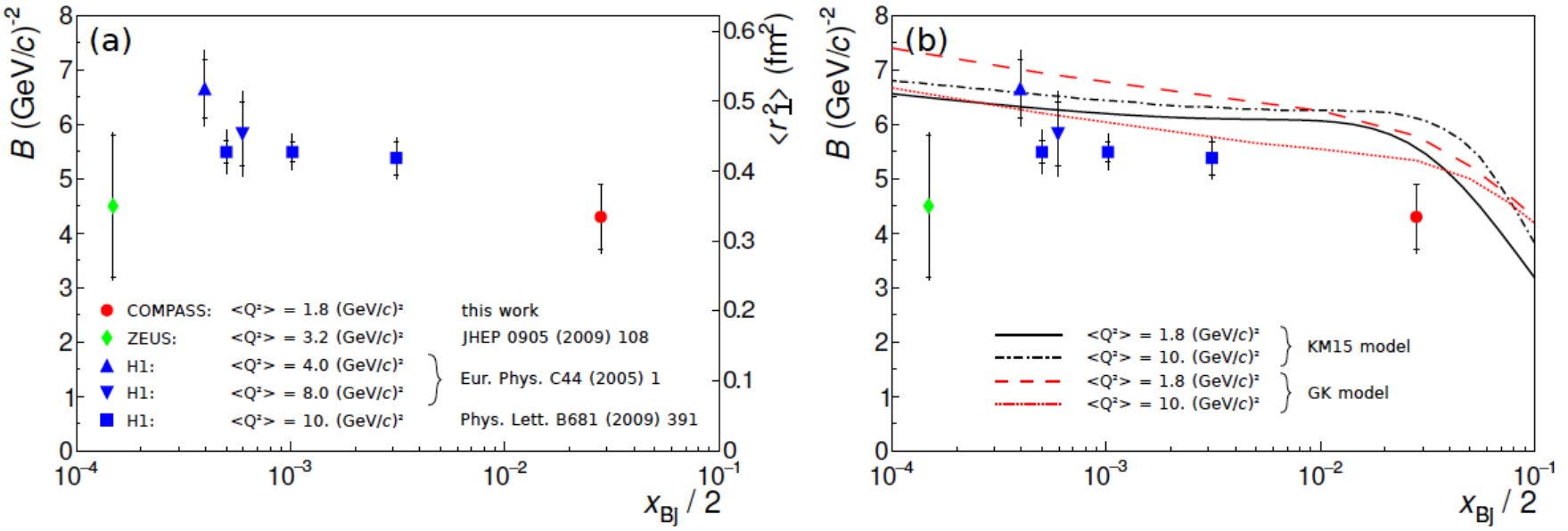

Figure 3: (a) Results from COMPASS and previous measurements by H1 [18] and ZEUS [19] on the t-slope parameter B, or equivalently the average squared transverse extension of partons in the proton, $\langle r_\perp^2 \rangle$, as probed by DVCS at the proton longitudinal momentum fraction $x_{\rm Bj}/2$ (see text). Inner error bars represent statistical and outer ones the quadratic sum of statistical and systematic uncertainties. (b) Same results compared to the predictions of the GK [20, 21, 17] and KM15 [22, 23] models. Figure is the corrected Fig. 5 from Ref. [7].

if substantiated, this could imply transverse expansion of dense gluonic state at low x and would impact saturation regime, maybe gluon density is reigned in that way! much better data needed to substantiate this.

now results from the JLAB CLAS experiment

see arXiv:1820.02110, 1902.02643

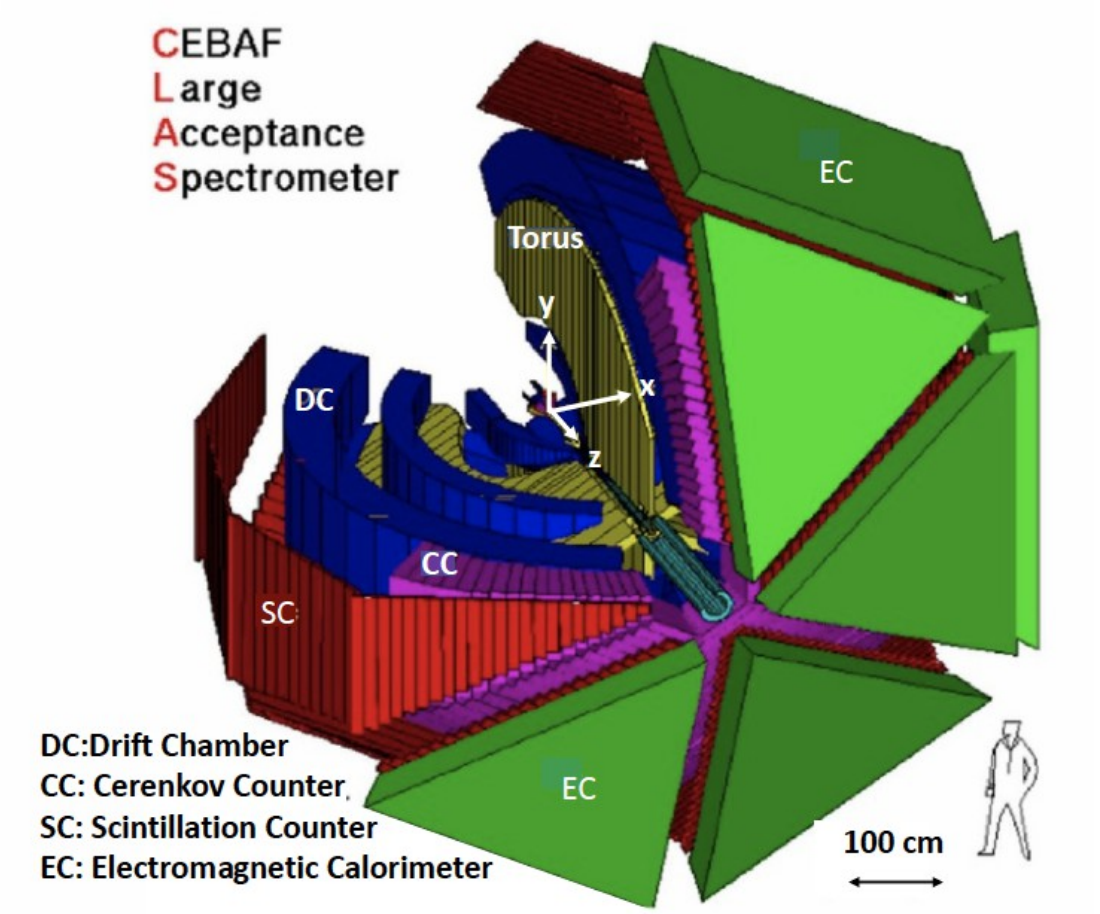

measure e p ⟶ e' p' γ
to determine
e' p' π

$$q(x,0,b_\perp) = \int \frac{d^2\Delta_\perp}{(2\pi)^2} e^{-ib_\perp \Delta_\perp} H^q(x,0,-\Delta_\perp^2)$$

$$t = \Delta^2 = (p'_N - p_N)^2$$

1st results on imaging in DVMP from CLAS

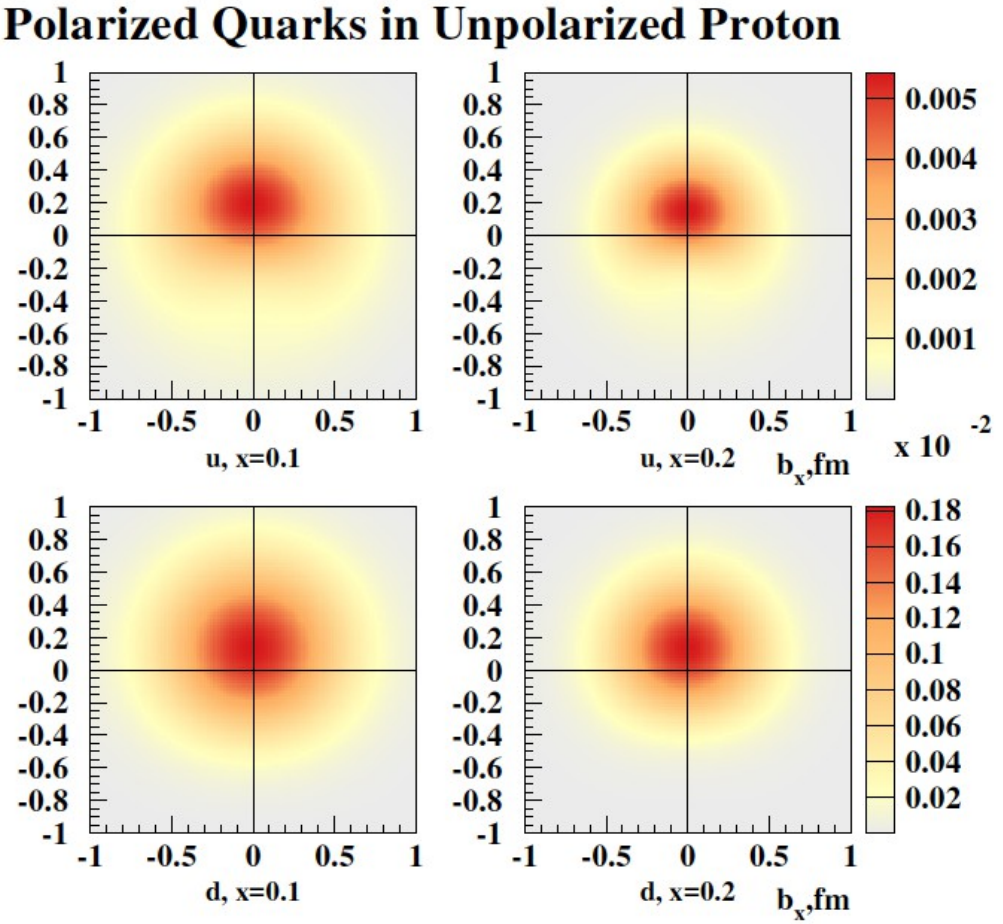

Figure 5: (Color online) Impact parameter density of quarks which are transversely polarized along b_x-axis in an unpolarized proton. Top left and right panels are for u-quarks with x=0.1 and x=0.2, respectively. Bottton left and right panels are for d-quarks with x=0.1 and x=0.2.

newest results from:
Gao and Vanderhaeghen, Rev. Mod. Phys. 94 (2022) 1, 015002
2105.00571 [hep-ph]

the following figure is taken from this paper

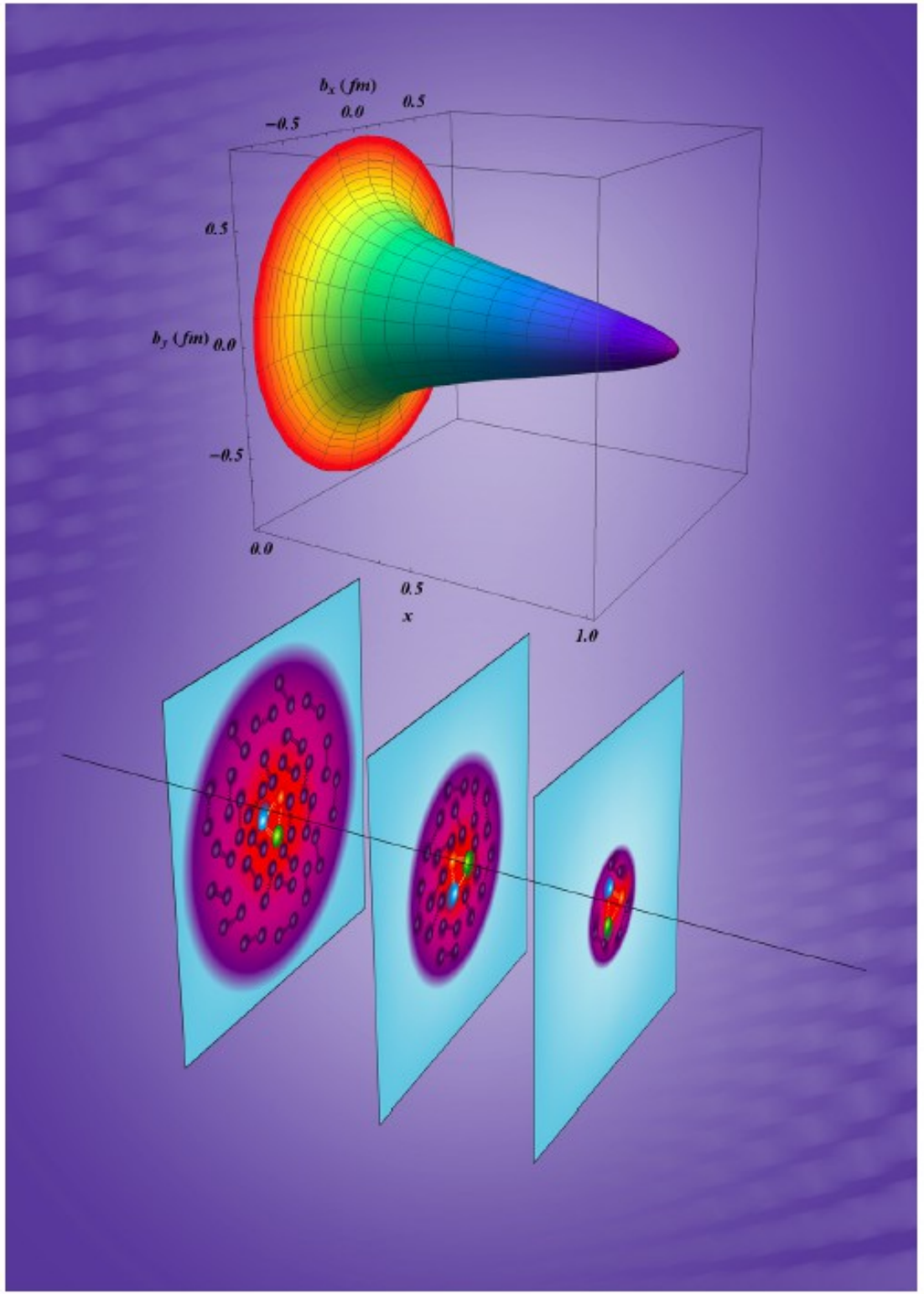

x-dependence of the protons transverse charge radfius

comment on the peculiar behavior of hadron masses

mass without mass: the (numerical) determination, within the framework of lattice QCD, of hadron masses. The figure is taken from:

Z. Fodor and C. Hoelbling,``Light Hadron Masses from Lattice QCD,"
Rev. Mod. Phys. 84 (2012), 449, arXiv:1203.4789 [hep-lat].

The u and d quarks have masses of a few MeV, the s quark has a mass of about 100 MeV, but the hadron masses are quantitatively reproduced.

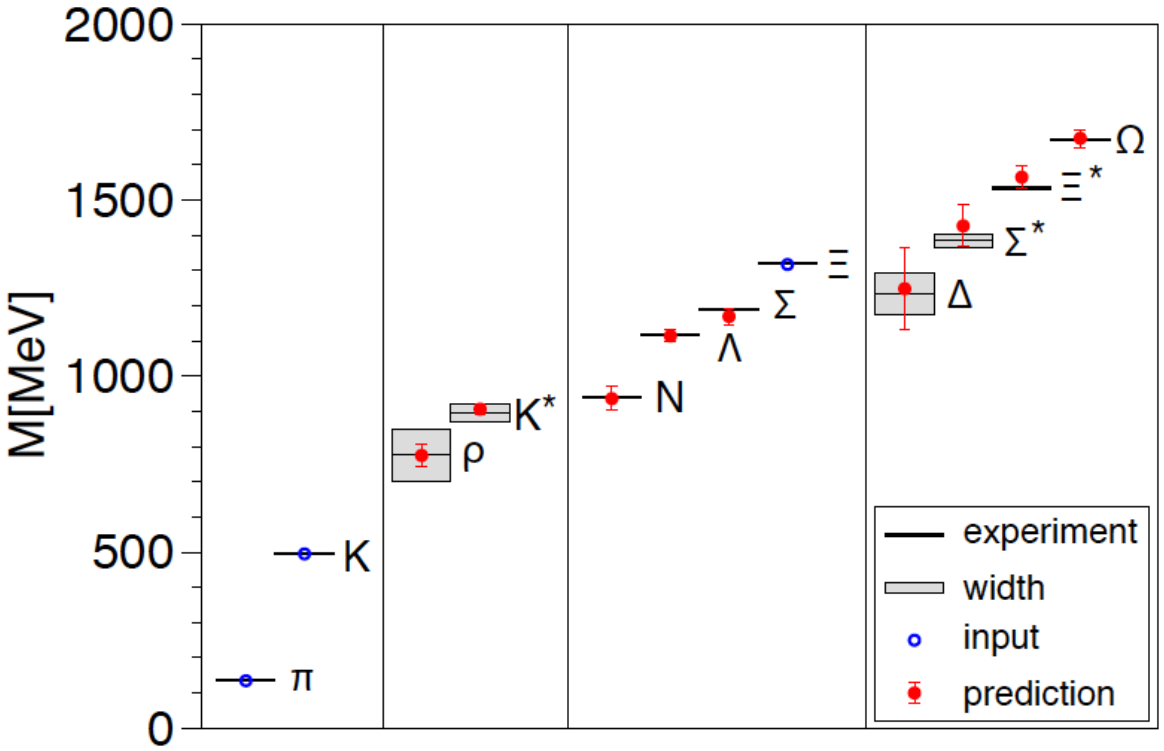

comment on the peculiar behavior of hadron masses

note:

an atom is bound by the electromagnetic potential between the positively charged nucleus and the surrounding electrons. but the total mass of the atom is smaller than the mass of the constituents. for hydrogen, m_p = 938.3 MeV, m_e = 0.511 MeV, but $M_H = (938.3 + 0.511 - 13.6\ 10^{-6})$ MeV.

a nucleus is bound by the interaction among the nucleons, the average binding energy is about 8 MeV per nucleon. so for a Pb nucleus with 208 nucleons, the total mass is approximately $M_{Pb} = (208 * 939 - 8 * 208)$ MeV, i.e. 1.7 GeV less than the sum of the masses of the constituents.

for the mass of a proton with m_p = 939 MeV, the masses of the constituents are m_u = 2.5 MeV, m_d = 5 MeV (see, e.g., 1809.07042), so the sum of the masses of the constituents is 10 MeV, about 1 % of the mass of the proton.